Available online at www.sciencedirect.com
SCIENCE DIRECT®
Journal of Chromatography A, 1096 (2005) 28–39
JOURNAL OF CHROMATOGRAPHY A
www.elsevier.com/locate/chroma

Probability theory for number of mixture components resolved by *n* independent columns

Joe M. Davis [a,*], Leonid M. Blumberg [b]

[a] *Department of Chemistry and Biochemistry, Southern Illinois University at Carbondale, Carbondale, IL 62901-4409, USA*
[b] *Fast GC Consulting, P.O. Box 585, Hockessin, DE 19707, USA*

Available online 13 May 2005

Abstract

A general theory is proposed for the probability of different outcomes of success and failure of component resolution, when complex mixtures are partially separated by *n* independent columns. Such a separation is called an *n*-column separation. An outcome of particular interest is component resolution by at least one column. Its probability is identified with the probability of component resolution by a single column, thereby defining the effective saturation of the *n*-column separation. Several trends are deduced from limiting expressions of the effective saturation. In particular, at low saturation the probability that components cluster together as unresolved peaks decreases exponentially with the number of columns, and the probability that components cluster together on addition of another column decreases by a factor equal to twice the column saturation. The probabilities of component resolution by *n*-column and two-dimensional separations also are compared. The theory is applied by interpreting three sets of previously reported retention indices of the 209 polychlorinated biphenyls (PCBs), as determined by GC. The origin of column independence is investigated from two perspectives. First, it is suggested that independence exists when the difference between indices of the same compound on two columns is much larger than the interval between indices required for separation. Second, it is suggested that independence exists when the smaller of the two intervals between a compound and its adjacent neighbors is not correlated with its counterpart on another column.

Keywords: *n*-Column separation; Multi-column separation; Statistical-overlap theory

1. Introduction

Several modifications of single-column separations have been made to increase resolution, when selectivity and efficiency are inadequate. Among these include the use of tandem columns, recycling, column switching, and multi-dimensional separations. A traditional approach is to use two or more columns of different selectivity, with the expectation that compounds of interest are separated by at least one of them. We are aware of only two theories that serve as guidelines to success. Both are probabilistic, with mixture components either randomly or uniformly distributed throughout the separations. Connors represented the *n* retardation factors of a compound in *n* TLC separations by an *n*-dimensional coordinate, which was distributed randomly among the discrete cells of an *n*-dimensional space. Each cell spanned one peak's width in all dimensions. He calculated the probability that cells contain either one or no coordinate, corresponding to total mixture resolution. He also calculated the probability that, on average, one cell contained more than one coordinate [1]. Martin et al. later calculated the probability of resolving all mixture components by at least one of *n* columns as the complement of the probability that separation by all *n* columns is incomplete. The probability was calculated from a general expression of the likelihood that a specific number of intervals (in this case, all of them) between adjacent, uniformly distributed peak centers exceeded the interval required for resolution [2]. Although the two theories differ in form, both depend on the number of mixture components, the number *n* of separations, and the separations' peak capacities. Both theories affirmed the probability of total mixture resolution increases with increasing column number. Specifically, Connors showed four TLC plates, each having a peak

* Corresponding author. Tel.: +1 618 453 6464; fax: +1 618 453 6408.
E-mail address: davis@chem.siu.edu (J.M. Davis).

0021-9673/$ – see front matter © 2005 Elsevier B.V. All rights reserved.
doi:10.1016/j.chroma.2005.03.137

capacity of 10, should be able to resolve about 100 components [1], and Martin et al. [2] showed the probability that a 10-component mixture is fully resolved increases from 20% to 89%, when the number of columns having a peak capacity of 50 increases from 1 to 10.

A common theme of both theories is complete or nearly complete resolution. In some cases, this is not required; rather, it is sufficient that the probability of separation be increased. In this paper, we propose general expressions for the probability that a mixture component is separated by n columns. The theory is applied by comparing its predictions to our interpretation of three recently reported sets of retention indices of polychlorinated biphenyls (PCBs), as measured by GC with three different stationary phases [3]. The numbers of the 209 congeners expected to be separated by the resolution threshold reported in ref. [3] – about 100 by any one column, 150 by any two columns, and 180 by the three columns – are consistent with calculations based on the indices.

2. Theory

2.1. Basics

Consider the partial separation of a mixture by n one-dimensional columns of different selectivity, henceforth to be called an n-column separation. Let p_i equal the probability that a mixture component is resolved as a singlet by the ith column, with $\bar{p}_i = 1 - p_i$ equaling the complementary probability that it is not resolved. In general, p_i differs for different columns, depending on specifics of the separation. We define a state as a member of the 2^n possible outcomes of success and failure of resolution by the n-column separation. If the p_i's are independent, then the probability that a state occurs can be calculated by multiplying appropriate values of p_i and $\bar{p}_i$.

For example, if $n = 2$, then $2^2 = 4$ states exist. If the two columns arbitrarily are labeled 1 and 2, then the states are: resolution by both 1 and 2, resolution by 1 but not 2, resolution by 2 but not 1, and resolution by neither 1 nor 2. For the independent probabilities p_1 and p_2, the state probabilities are p_1p_2, $p_1\bar{p}_2$, $\bar{p}_1p_2$, and $\bar{p}_1\bar{p}_2$, respectively. They sum to one, as is verified by substituting expressions for the complementary probabilities. Different states are generalized easily as n increases, since they are analogous to the output states of an n-bit analog-to-digital converter (hence, our designation of the 2^n outcomes as states), and their probabilities are evaluated simply. Table 1 reports the eight states and their probabilities for $n = 3$. As before, the probabilities sum to one.

Since components of singlet peaks (singlets) are more easily identified and quantified than those of multiplets, the probability that a component is separated by at least one column is of particular interest. For n columns, this outcome occurs in $2^n - 1$ states; the only state in which it does not corresponds to failure of separation by all n columns. The probability $p(n)$ of separation by at least one column consequently is the complement of the probability that separation occurs on no column

$$p(n) = 1 - \prod_{i=1}^{n} \bar{p}_i \quad (1)$$

where the capital pi indicates that n $\bar{p}_i$ factors are multiplied. In mathematical form, Eq. (1) is identical to the equation reported by Martin et al. [2]. We are interested, however, in the probability that only a single component is resolved, instead of the probability of total resolution (i.e., the $\bar{p}_i$ factors differ in the two equations). Eq. (1) represents the sum of all state probabilities, except the one associated with complete failure of resolution. For example, the sum of p_1p_2, $p_1\bar{p}_2$, and $\bar{p}_1p_2$ equals $p(2)$ for a 2-column separation, and the sum of the first seven states in Table 1 equals $p(3)$ for a 3-column separation. Since $p(n)$ is the sum of all state probabilities, except one, it is greater than any p_i and the likelihood of component separation increases.

Table 1
States and state probabilities for three columns labelled 1, 2, and 3

State			State probability
1	2	3	
+	+	+	$p_1p_2p_3$
+	+	−	$p_1p_2\bar{p}_3 = p_1p_2 - p_1p_2p_3$
+	−	+	$p_1\bar{p}_2p_3 = p_1p_3 - p_1p_2p_3$
−	+	+	$\bar{p}_1p_2p_3 = p_2p_3 - p_1p_2p_3$
+	−	−	$p_1\bar{p}_2\bar{p}_3 = p_1 - p_1p_3 - p_1p_2 + p_1p_2p_3$
−	+	−	$\bar{p}_1p_2\bar{p}_3 = p_2 - p_2p_3 - p_1p_2 + p_1p_2p_3$
−	−	+	$\bar{p}_1\bar{p}_2p_3 = p_3 - p_2p_3 - p_1p_3 + p_1p_2p_3$
−	−	−	$\bar{p}_1\bar{p}_2\bar{p}_3 = 1 - p_1 - p_2 - p_3 + p_1p_2 + p_1p_3 + p_2p_3 - p_1p_2p_3$

Singlet probabilities for individual columns are p_1, p_2, and p_3, respectively. Pluses and minuses indicate resolution and failure of resolution, respectively.

Both the state probabilities and Eq. (1) are general and not constrained by a specific type of probability distribution. In subsequent discussion, we will assume that mixture components are randomly distributed throughout separations but this is not necessary. However, all probabilities p_i must be independent, and this is discussed later.

2.2. Relations between singlet probabilities in single- and n-column separations

The probability $p(n)$ can be interpreted directly, but it is instructive to relate it to statistical-overlap theory (SOT), on which several reviews have been published [4–7]. In SOT, a separation is postulated to be one of a large ensemble of similar separations, in which the number of mixture components and their retention times (or other measure of positions) vary in accordance with some probability distribution and fre-

quency. In the simplest theory, the components are randomly distributed in accordance with a homogeneous Poisson process, and the probability p_i of singlet formation in the ith separation is [8].

$$p_i = \mathrm{e}^{-2\alpha_i} = \mathrm{e}^{-2\bar{m}/n_{\mathrm{c},i}} \tag{2}$$

where $\bar{m}$ is the average number of mixture components in the separation ensemble, and α_i and $n_{\mathrm{c},i}$ are the saturation and peak capacity. The probability p_i is increased by reducing saturation α_i.

In an n-column separation, it suffices that a component is resolved, regardless of the number of columns resolving it. Because all states contributing to separation are relevant, we propose that $p(n)$ in Eq. (1) be identified with a specific form of Eq. (2).

$$p(n) \equiv \mathrm{e}^{-2\alpha_\mathrm{e}(n)} \tag{3}$$

where $\alpha_\mathrm{e}(n)$ is the saturation of a single-column separation having the same effective singlet probability as an n-column separation.

This interpretation facilitates derivation of relations connecting the two separation types. By combining Eqs. (1)–(3), we explicitly can write

$$\mathrm{e}^{-2\alpha_\mathrm{e}(n)} = 1 - (1 - \mathrm{e}^{-2\alpha_1})(1 - \mathrm{e}^{-2\alpha_2}) \ldots (1 - \mathrm{e}^{-2\alpha_{n-1}})(1 - \mathrm{e}^{-2\alpha_n}) \tag{4a}$$

which determines $\alpha_\mathrm{e}(n)$ as

$$\alpha_\mathrm{e}(n) = -\tfrac{1}{2}\ln[1 - (1 - \mathrm{e}^{-2\alpha_1})(1 - \mathrm{e}^{-2\alpha_2}) \ldots (1 - \mathrm{e}^{-2\alpha_{n-1}})(1 - \mathrm{e}^{-2\alpha_n})] \tag{4b}$$

2.3. Limiting cases

Several insights are obtained by considering limiting cases of Eqs. (3) and (4b). If the saturations of the n columns are the same (i.e., if the columns have the same peak capacity), then all p_i's are equal and Eq. (4b) reduces to

$$\alpha_\mathrm{e}(n) = -\tfrac{1}{2}\ln[1 - (1 - \mathrm{e}^{-2\alpha})^n] \tag{5}$$

where $\alpha = \alpha_i$ for all columns. For small α, Taylor-series expansions can be used to simplify Eq. (5)

$$\alpha_\mathrm{e}(n) \approx 2^{n-1}\alpha^n;\ 0 < \alpha \ll 1 \tag{6a}$$

for which Eq. (3) predicts the singlet probability $p(n)$ to be

$$p(n) \approx \mathrm{e}^{-(2\alpha)^n} \approx 1 - (2\alpha)^n; \quad 0 < \alpha \ll 1 \tag{6b}$$

Eq. (6b) shows that $p(n)$ rapidly approaches one with decreasing α and increasing n.

However, for small α, $p(n)$ already might be close to one, even for a single column. Since it cannot exceed one, it only can increase slightly with increasing n. Eq. (6b) consequently does not tell the full story of the improvement of separation made possible by n-column separations. Rather, the improvement is conveyed better by the reduction of the cluster probability $\bar{p}(n)$, which is the probability that a component is not a singlet but is part of a doublet peak, triplet peak, etc. From Eqs. (1) and (6b), one easily calculates

$$\bar{p}(n) = 1 - p(n) = \prod_{i=1}^{n} \bar{p}_i \approx (2\alpha)^n; \quad 0 < \alpha \ll 1 \tag{6c}$$

Eq. (6c) shows that the cluster probability decreases as a power of the number n of columns. Furthermore, the smaller α is, the more rapid is the decrease with increasing n.

In contrast, for large α, direct expansion of Eq. (5) gives the approximation

$$\alpha_\mathrm{e}(n) \approx -\tfrac{1}{2}\ln(n) + \alpha; \quad \alpha \gg 1 \tag{7a}$$

for which the singlet probability is

$$p(n) \approx n\mathrm{e}^{-2\alpha} = np_i; \quad \alpha \gg 1 \tag{7b}$$

Thus, for large α, an n-column separation provides only an n-fold increase of the singlet probability associated with any column. Clearly, the potential of n-column separations to improve resolution is largest at small α.

2.4. Effect of additional column

Since one's first approach to improving an n-column separation might be to add another column, the decrease of cluster probability and increase of singlet probability resulting from this action are of interest. These can be calculated from

$$\frac{\bar{p}(n-1)}{\bar{p}(n)} = \frac{\prod_{i=1}^{n-1}\bar{p}_i}{\prod_{i=1}^{n}\bar{p}_i} = \frac{1}{\bar{p}_n} = (1 - \mathrm{e}^{-2\alpha_n})^{-1}; \quad n \geq 2 \tag{8a}$$

and

$$\frac{p(n)}{p(n-1)} = \frac{1 - \prod_{i=1}^{n}\bar{p}_i}{1 - \prod_{i=1}^{n-1}\bar{p}_i}; \quad n \geq 2 \tag{8b}$$

where both ratios are greater than 1. Although Eqs. (8a) and (8b) are equally valid, the former provides more useful insights at small α and the latter at large α. This happens, because $p(n)$ and $\bar{p}(n)$ are almost one at small and large α, respectively, and the ratio of two such quantities having n values differing by only the number, one, is not very informative.

At small α, Eq. (8a) can be simplified by Taylor-series expansion to

$$\frac{\bar{p}(n-1)}{\bar{p}(n)} \approx (2\alpha_n)^{-1}; \quad 0 < \alpha_n \ll 1, n \geq 2 \tag{9a}$$

Eq. (9a) is a logical consequence of Eq. (6c), when all α_i are equal. It also is valid even when they are not equal, since all $\bar{p}_i$ factors in Eq. (8a) except $\bar{p}_n$ cancel. In contrast, substitution

of Eq. (7b) into Eq. (8b) reveals

$$\frac{p(n)}{p(n-1)} \approx \frac{n}{n-1}; \quad \alpha \gg 1, n \geq 2 \tag{9b}$$

Eq. (9a) shows that addition of another column at low α_n and low cluster probability (high singlet probability) dramatically reduces the likelihood that a clustered or unresolved peak exists. The reduction is independent of the number of columns but increases rapidly with decreasing α_n. In contrast, Eq. (9b) shows that addition of another column at large α, unsurprisingly, is not very effective. For example, the singlet probability in a 2-column separation is only two times larger than in a single-column separation. Also, the degree of improvement decreases with addition of each extra column and is independent of α.

2.5. Relation between singlet probabilities in n-column and two-dimensional separations

SOT also exists for separations in two [9–11] and higher [12,13] dimensions. In light of interest in comprehensive two-dimensional gas chromatography (GC × GC) [14–17], liquid-chromatography/capillary electrophoresis (LC × CE) [18–21], and related methodologies, we compare the singlet probability p_{2D} in a two-dimensional separation to that of an n-column separation. For a large rectangular space containing zones having equal standard deviations in both dimensions, the former can be expressed as [22]

$$p_{2D} = e^{-\alpha_1 \pi / n_c^*} \tag{10}$$

where α_1 is the saturation of the first dimension and n_c^* is the peak capacity of the orthogonal second dimension (corrections to p_{2D} for small spaces and unequal standard deviations were made recently [11]). The general comparison is made by equating Eqs. (4a) and (10). For the special case in which the saturations of the n columns and the first dimension of the two-dimensional separation are the same and equal to α, this relation simplifies to

$$e^{-\alpha\pi/n_c^*} = 1 - (1 - e^{-2\alpha})^n \tag{11}$$

which determines n_c^* for different α and n. Eq. (11) is a logical basis of comparison, since it rests on the assumption that the first separation is the same in the two separation types and quantifies the n_c^* necessary to equal the increased singlet probability provided by $n-1$ additional columns. Similar relations can be derived for higher dimensions.

2.6. Expected numbers of components associated with given probability

The expected number of components in a specific state and the expected numbers of components resolved by a single column, an n-column separation, or a two-dimensional separation are equal to the product of $\bar{m}$ and the appropriate probability (e.g., p_i, $p(n)$, etc.).

2.7. Alternative theory for p_i

In some cases, Eq. (2) is too simple to describe the singlet probability and must be replaced by [23,24]

$$p_i = \int_0^1 f(\zeta) e^{-2\alpha(\zeta)}\, d\zeta \tag{12a}$$

where ζ is a reduced time (or volume, index, etc.) spanning zero to one, $f(\zeta)$ is the frequency of reduced retention times, and the saturation

$$\alpha(\zeta) = \frac{\bar{m} f(\zeta) x_0(\zeta)}{X} \tag{12b}$$

varies with ζ (the subscript, i, is not used with most terms in Eq. (12) for the sake of simplicity). In Eq. (12b), $x_0(\zeta)$ is the minimum interval between successive retention times required for separation, which often varies with ζ due to changes of peak width and resolution [24], and X is the span of the separation. The frequency $f(\zeta)$, which is a probability density function having unit area, accounts for the inhomogeneity of retention times, i.e., the elution of significantly different numbers of mixture components, within the same time interval, in different regions of the separation. If $x_0(\zeta) \equiv x_0$ is constant and $f(\zeta) = 1$, then Eq. (12) reduces to Eq. (2), since X/x_0 is the peak capacity. Detailed explanations of the principles underlying Eq. (12), which can be substituted for $e^{-2\alpha_i}$ in the preceding equations, are given elsewhere [23,25].

3. Procedures

3.1. Computer simulations

Digital simulations were carried out to verify state probabilities and Eq. (1) for mimicked 2- and 3-column separations. For various p_i's and $\bar{m}$'s, mimicked mixture components were assigned to different states based on successes and failures of separation, as determined by random numbers less than p_i and greater than p_i, respectively. From 500 such simulations, the average and standard deviation of the numbers of components in each state, and separated by at least one column, were computed. These were compared to theoretical expectations and reduced chi-squares were calculated. In the simulations, the p_i's varied over the 19 values, 0.05, 0.10, 0.15..., 0.90, and 0.95, and all p_i combinations were considered ($19^2 = 361$ for $n = 2$; $19^3 = 6859$ for $n = 3$). The $\bar{m}$'s were 50, 250, and 500, with the actual Poisson distributed number of mimicked components in any simulation approximated by the Box–Muller transform [26].

3.2. Analysis of PCB data

Three sets of retention indices of the 209 PCBs, reported in ref. [3] and determined by GC with three cap-

illary columns, were interpreted by theory. The columns were 60 m × 0.25 mm i.d., with a 0.25 μm film of DB-XLB; 60 m × 0.25 mm i.d., with a 0.10 μm film of DB-5; and 30 m × 0.25 mm i.d., with a 0.25 μm film of DB-17MS. They were held at 50 °C for 2 min and then ramped to 300 °C at 2 °C/min. Other chromatographic details are found in the reference [3]. The frequencies $f(\zeta)$ of the indices were computed with the software, Minitab Release 12 for Windows (Minitab, Inc., State College, PA). For each column, probability p_i was calculated from Eq. (12) using $f(\zeta)$ and Simpson's rule, with $\bar{m}$ and x_0 equaling 209 and one index unit, respectively. The expected numbers of PCBs in different states, and separated by at least one column, were predicted from these p_i's for three 2-column separations based on DB-XLB and DB-5, DB-XLB and DB-17MS, and DB-5 and DB-17MS, and for the one 3-column separation. The predictions were compared to the numbers of PCBs identified as singlets in ref. [3], based on the assumption that one index unit sufficed for resolution. Different congeners were identified by IUPAC numbers, and only congeners having unique IUPAC numbers were counted in determining the number of singlets.

The predictions then were generalized by repeating the calculations for different x_0 values and interpreting the index tables. In the interpretations, a PCB was identified as a singlet if its index was separated from the indices of the previous and subsequent PCBs by at least x_0 index units. As before, different congeners were identified by IUPAC numbers.

The differences between the indices of the same congener on different columns, and the variation among different columns of the smaller of the two intervals between a congener and its adjacent neighbors, were calculated to characterize the independence of the PCB p_i's. To assist the characterization, the retention indices of congeners were simulated with random numbers in agreement with frequency $f(\zeta)$, using procedures discussed elsewhere [23,24].

3.3. Computations

All computational algorithms were written in FORTRAN 90 or Mathematica 4.0 (Wolfram Research, Inc., Champaign, IL).

4. Results and discussion

4.1. Validation by simulation

Table 2 reports the reduced chi-squares χ^2_ν calculated from digital simulations carried out to verify theory for different state probabilities and Eq. (1). They are less than 0.01 and signify the correctness of theory. Two trends are that χ^2_ν decreases slightly with increasing $\bar{m}$ and is larger for $p(n)$ than for individual state probabilities. In all cases, however, theory is sound.

Table 2
Reduced chi-squares χ^2_ν calculated from digital simulations and theory

n	Probability	$\chi^2_\nu \times 10^3$		
		$\bar{m} = 50$	$\bar{m} = 250$	$\bar{m} = 500$
2	p_1p_2	2.84	2.14	2.12
	$p_1\bar{p}_2$	3.53	2.29	2.25
	$\bar{p}_1p_2$	3.29	2.56	1.88
	$\bar{p}_1\bar{p}_2$	3.23	2.37	2.39
	$p(2)$	5.57	2.77	2.17
3	$p_1p_2p_3$	2.70	2.11	2.01
	$p_1p_2\bar{p}_3$	2.65	2.03	2.03
	$p_1\bar{p}_2p_3$	2.66	2.16	2.08
	$\bar{p}_1p_2p_3$	2.65	2.25	2.01
	$p_1\bar{p}_2\bar{p}_3$	2.68	2.11	2.08
	$\bar{p}_1p_2\bar{p}_3$	2.78	2.19	2.09
	$\bar{p}_1\bar{p}_2p_3$	2.69	2.20	2.07
	$\bar{p}_1\bar{p}_2\bar{p}_3$	2.63	2.21	2.07
	$p(3)$	6.38	2.88	2.46

$\nu = 361$ for $n = 2$ and 6859 for $n = 3$.

4.2. Implications

Fig. 1 is a graph of $\alpha_e(n)$ versus α, for $n = 1, 2, 3, 5$, and 10, as calculated from Eq. (5). The bold line represents $\alpha_e(n) = \alpha$ for a single column ($n = 1$). All other graphs lie below the line, indicating that $\alpha_e(n) < \alpha$ and the singlet probability increases with column number. The dashed lines represent the approximation, Eq. (7a), and coincide with the curves at large α, which have the limiting slope of one. The insert is an expansion of the lower left-hand corner of Fig. 1. The dashed curves represent the approximation, Eq. (6a), whose relative error at any α increases with increasing n. Of particular interest is its prediction of the rate at which $\alpha_e(n)$ increases with small α

$$\frac{d\alpha_e(n)}{d\alpha} \approx n(2\alpha)^{n-1}; \quad 0 < \alpha \ll 1 \tag{13}$$

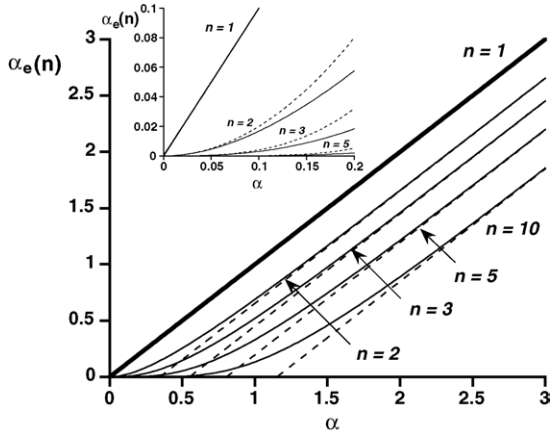

Fig. 1. Graph for different n of saturation $\alpha_e(n)$ defining singlet probability of an n-column separation vs. saturation α of single-column separation. Insert is expansion of graph at low α. Dashed curves and lines represent limiting approximations.

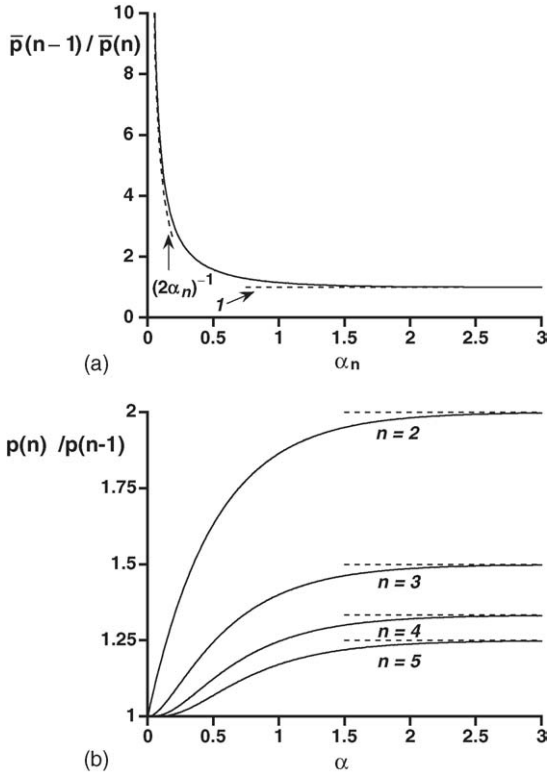

Fig. 2. (a) Graph of cluster probability ratio $\bar{p}(n-1)/\bar{p}(n)$ vs. saturation α_n of the nth separation. (b) Graph of singlet probability ratio $p(n)/p(n-1)$ vs. α for different n.

which is small for large n. Since $\alpha_e(n) = 0$ at $\alpha = 0$, Eq. (13) implies that $\alpha_e(n)$ differs little from zero for large n and small α. For example, $\alpha_e(5) = 0.00195$ for $\alpha = 0.2$, corresponding to an increase of singlet probability from $p(1) = 0.670$ to $p(5) = 0.996$. In contrast, for the same α, $\alpha_e(2)$ only decreases to 0.0575 and $p(2)$ only increases to 0.891. Clearly, if a single-column separation is fairly good (i.e., if α is small) and columns behave independently, then introducing a few additional columns having similar saturations almost guarantees component resolution in at least one separation.

The linear dependence of $p(n)$ on n at large α (Eq. (7b)) is explained easily. For large α, all probabilities p_i are small, their products (e.g., $p_i p_j$, $i \neq j$) are negligibly small, and only the n states corresponding to separation by a single column are relevant. This is easily understood by considering the first seven states in Table 1, which contribute to $p(3)$. Only the three state probabilities $p_1\bar{p}_2\bar{p}_3$, $\bar{p}_1 p_2 \bar{p}_3$, and $\bar{p}_1\bar{p}_2 p_3$ contain terms p_i that are not multiplied by other probabilities. At large α, $p(3) \approx p_1 + p_2 + p_3$, which generalizes to np_i for equal p_i.

Fig. 2a is a graph of the cluster probability ratio $\bar{p}(n-1)/\bar{p}(n)$ versus α_n. At large α_n, the ratio approaches one, as represented by the dashed horizontal line. Here, overlap is so severe that the nth column scarcely affects the cluster probability. At small α_n, however, $\bar{p}(n-1)$ is much larger than $\bar{p}(n)$, and their ratio approaches the limit $(2\alpha_n)^{-1}$ (Eq. (9a)) represented by the dashed curve. The importance of this finding should be emphasized. In practice, method developers may spend inordinate amounts of time trying to separate a few unresolved peaks, when a separation of small saturation is otherwise acceptable. Fig. 2a shows that the probability of having unresolved peaks at small saturation declines rapidly with *each* addition of a new column. Consequently, the addition of another column may provide more effective means of increasing resolution than modifying the existing separation.

Fig. 2b is a graph of the singlet probability ratio $p(n)/p(n-1)$ versus α for $n = 2$, 3, 4, and 5, when all column saturations $\alpha_i \equiv \alpha$ are equal. At small α, the ratio rapidly increases for $n = 2$ but increases more slowly for large n. This outcome occurs, because $p(n)$ approaches one for small α and large n, and simply cannot increase more. Between $\alpha = 1$ and 2, $p(n)/p(n-1)$ approaches the limiting values predicted by Eq. (9b), which are represented by the dashed horizontal lines. Although $p(n)/p(n-1)$ maximizes at large α, this has little significance. Separations at large α are poor, and it matters little that an n-column separation is slightly better than one based on $n-1$ columns.

The attainment of acceptable levels of peak capacity and saturation by a single-column separation must be balanced against the requirements of analysis time and linear range. Potentially, they also can be attained without compromising these requirements by using comprehensive multi-dimensional separations [14–21]. Of particular interest is comprehensive two-dimensional gas chromatography (GC × GC). It has been shown elsewhere [15] that the potential peak-capacity gain G in *optimized* GC × GC, as compared to *optimized* single-column GC based on the same first-dimension column, can be estimated as $G \approx 0.13 N_1^{1/3}/R_{s,2,min}$, where N_1 is the plate number of the first-dimension column and $R_{s,2,min}$ is the minimal acceptable resolution in the second dimension. For typical first-dimension columns and $R_{s,2,min} = 1$, the addition of a second dimension can result in a potential order of magnitude increase in total peak capacity. However, at the current state of the art, several aspects of GC × GC must be improved substantially [15] to realize this potential capacity. Most notably, the width of the modulator pulse must be reduced, without loss of analyte, by about an order of magnitude. Furthermore, the standard deviation of the modulator pulse should be smaller than 5 ms, while known cryogenic modulators that preserve analyte have standard deviations greater than 25 ms [27,28]. As a result, even the parity of saturation in currently available GC × GC systems and their optimized single-column counterparts can be questioned [29,30], and n-column separations – especially dual-column ones – remain the only practical way to reduce saturation without compromising analysis time and linear range. However, we are confident that these technical problems will be solved eventually, and consequently we compare the performance of n-column separations to two-dimensional ones like GC × GC.

Fig. 3 is a graph of log n_c^* versus α for $n = 2$, 3, 5, and 10, as calculated from Eq. (11) by numerical bisection. Suppose that second-dimension peak capacities n_c^* in comprehensive

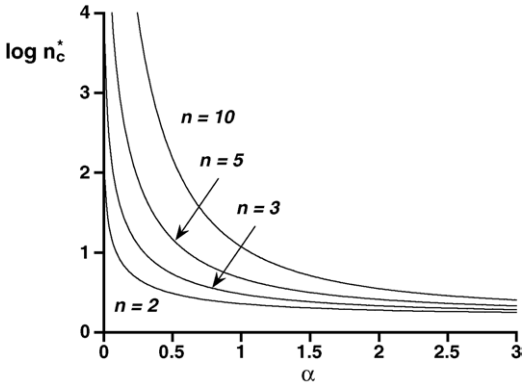

Fig. 3. Graph of log n_c^* vs. α for different n, where n_c^* is the second-dimension peak capacity required for two-dimensional and n-column separations to have same the singlet probability. The α's of the first dimension of the two-dimensional separation and all n columns are the same.

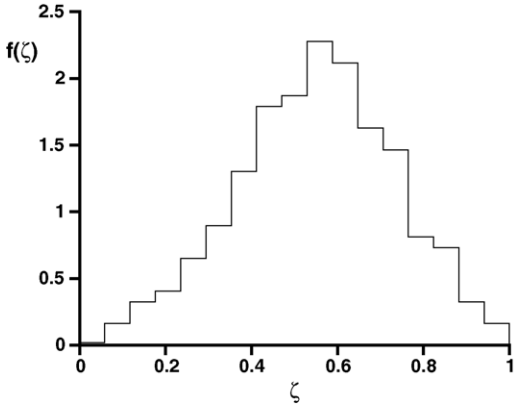

Fig. 4. Graph of frequency $f(\zeta)$ of reduced retention indices vs. reduced retention index ζ of 209 PCBs measured on DB-XLB stationary phase. Indices are reported in ref. [3].

two-dimensional separations lie between 10 and 100 (i.e., log n_c^* lies between 1 and 2). If the saturation α of the first dimension of the two-dimensional separation is large, then the value of n_c^* required to equal the singlet probability of an n-column separation easily is attained or exceeded, even for large n. This outcome reflects conditions where each of the n one-dimensional separations is relatively poor and the probability of separation is relatively small. Under these conditions, two-dimensional separations always will be superior to n-column separations. With decreasing α, however, Fig. 3 shows that it might be difficult or impossible to attain an n_c^* providing the same singlet probability as an n-column separation. This is a conclusion we anticipate to be controversial, but it is rationalized easily. *All* of the $2^n - 1$ states leading to resolution contribute favorably to an n-column separation, and the likelihood of separation increases with n. In contrast, if resolution must be achieved by a *single* two-dimensional separation, then at low α very stringent demands are placed on n_c^*. Perhaps it would be better to compare an n-column separation to n two-dimensional separations, instead of just one, but we defer that to another study.

4.3. Application of theory to PCB separations

Fig. 4 is a graph of frequency $f(\zeta)$ versus ζ computed from the retention indices (or simply indices) of the 209 PCBs measured on DB-XLB stationary phase, as reported in ref. [3]. The reduced indices $\zeta = 0$ and 1 correspond to the index bounds of 25 and 875, respectively, as calculated by the Minitab software. For statistical reasons [25], the bounds lie slightly beyond the actual first and last indices (33.0 and 867.0). All reduced indices are scaled linearly between the bounds. As shown in ref. [3], the indices vary linearly with time; consequently, so does ζ. The area, $f(\zeta)\,d\zeta$, is the probability that reduced indices lie between ζ and $\zeta + d\zeta$ [23,25]. Consequently, large $f(\zeta)$ values result when indices are closely grouped, i.e., when many PCBs elute in a brief time interval. Because volatility decreases with increasing chlorine number, the variation of $f(\zeta)$ with ζ largely follows the distribution of isomeric substitutions of chlorine on the biphenyl moiety, with a few low chlorine-substituted PCBs at the separation's beginning, a few high chlorine-substituted PCBs at the separation's end, and many intermediate chlorine-substituted PCBs between them. The frequencies of the other two separations are similar, differing only in small details. Because $f(\zeta)$ is markedly inhomogeneous, Eq. (12) must be used to calculate the singlet probability p_i for any column, instead of Eq. (2).

The numbers of PCBs resolved by a single index unit on the DB-XLB, DB-5, and DB-17MS columns are counted easily in Table 3 of ref. [3] (the unresolved ones conveniently are boxed) and are 115, 95, and 105, respectively. These numbers compare favorably to the expected numbers of singlets predicted by Eq. (12), which are 100.1 ($p_i = 0.4789$), 104.7 ($p_i = 0.5010$), and 104.0 ($p_i = 0.4976$), respectively. The differences of prediction are due to small differences in $f(\zeta)$. The variation of $f(\zeta)$ affects peak overlap significantly; if we were to use Eq. (2) instead of Eq. (12), we would overpredict the expected numbers of singlets as 127.8, 131.4, and 127.8, respectively. Although the predictions are good, they are not exact. Pietrogrande et al. [31] have shown that Arochlors, or specific mixtures of PCBs, produce intervals between adjacent indices (actually, retention times) that are increasingly structured as the chlorine content increases. We shall use the Poisson distribution, however, because the error for PCBs is small, both here and in previous assessments based on GC-simulation software [24,25,32].

Table 3 reports the expected and actual numbers of PCBs resolved by one index unit for various separation outcomes. The expected numbers were calculated from state probabilities and Eq. (1) using both p_i's evaluated by SOT and empirical probabilities calculated from the indices (e.g., for DB-XLB, 115 singlets are found, so the actual singlet probability is 115/209 = 0.5502). The latter calculations avoid any bias caused by SOT and assess independently if the congeners resolved by different combinations of columns are behav-

Table 3
Expected and actual numbers of resolved PCBs in different states of 2- and 3-column separations

DB-XLB	DB-5	Number	Expected number, theory	
			SOT	Empirical
+	+	60	50.1	52.3
+	–	55	50.0	62.7
–	+	35	54.5	42.7
–	–	59	54.4	51.3
Resolved by at least one of two columns		150	154.6	157.7

DB-XLB	DB-17MS	Number	Expected number, theory	
			SOT	Empirical
+	+	61	49.8	57.8
+	–	54	50.3	57.2
–	+	44	54.1	47.2
–	–	50	54.7	46.8
Resolved by at least one of two columns		159	154.3	162.2

DB-5	DB-17MS	Number	Expected number, theory	
			SOT	Empirical
+	+	51	52.1	47.7
+	–	44	52.6	47.3
–	+	54	51.9	57.3
–	–	60	52.4	56.7
Resolved by at least one of two columns		149	156.6	152.3

DB-XLB	DB-5	DB-17MS	Number	Expected number, theory	
				SOT	Empirical
+	+	+	34	24.9	26.3
+	+	–	26	25.2	26.0
+	–	+	27	24.9	31.5
–	+	+	17	27.1	21.5
+	–	–	28	25.1	31.2
–	+	–	18	27.4	21.3
–	–	+	27	27.0	25.8
–	–	–	32	27.3	25.5
Resolved by at least one of three columns			177	183.5	181.7

Expected numbers were evaluated from p_i's calculated by SOT and determined empirically. Actual numbers were determined from indices in ref. [3]. Pluses and minuses indicate resolution and failure of resolution, respectively. $x_0 = 1$ index unit.

ing in a statistical manner. The actual numbers of singlets correspond to all resolved congeners having unique IUPAC numbers (i.e., a congener was counted only once, no matter how many times it was resolved). Overall, a good agreement exists between the expected and actual numbers of resolved PCBs in the different states of the *n*-column separations, regardless of how theory is calculated. The calculations based on empirical probabilities are superior in some cases, especially when small errors in predictions by SOT reinforce one another. For example, the state probability is overpredicted for failed resolution by DB-XLB and successful resolution by DB-5 (first sub-table, third row), because the predicted $\bar{p}_i$ for DB-XLB is high (i.e., the predicted p_i is low) and the predicted p_i for DB-5 is high. Consequently, these two positive errors reinforce on multiplication. In other cases, however, predictions based on SOT probabilities are superior to empirical ones. Most important, the predictions based on $p(n)$ are excellent in all cases. The sum of both the expected and actual numbers of PCBs in all states is 209, the total number of PCBs. By happenstance, the expected numbers of PCBs in all states of the 2-column separations and all states of the 3-column separation are about the same, because all p_i's and $\bar{p}_i$'s are about 0.5. As predicted, the increase of singlet number due to supplementing two columns by a third one (i.e., from 149–159 singlets to 177) is smaller than the increase due to supplementing a single column by a second one (i.e., from 95–115 singlets to 149–159). Together, the three columns resolve $(177/209) \times 100 \approx 85\%$ of the PCBs, whereas any one column resolves only about 50% of them.

In addition to these results, the expected numbers $\bar{m}\,p(n)$ of PCB singlets resolved by at least one column were predicted for other intervals x_0 and compared to the numbers actually found on further interpreting the three sets of retention indices. Fig. 5 is a graph of these numbers versus $\bar{m}x_0/X$, with $\bar{m} = 209$ and X equaling the separations' span in retention indices, as predicted by Minitab software. Because the

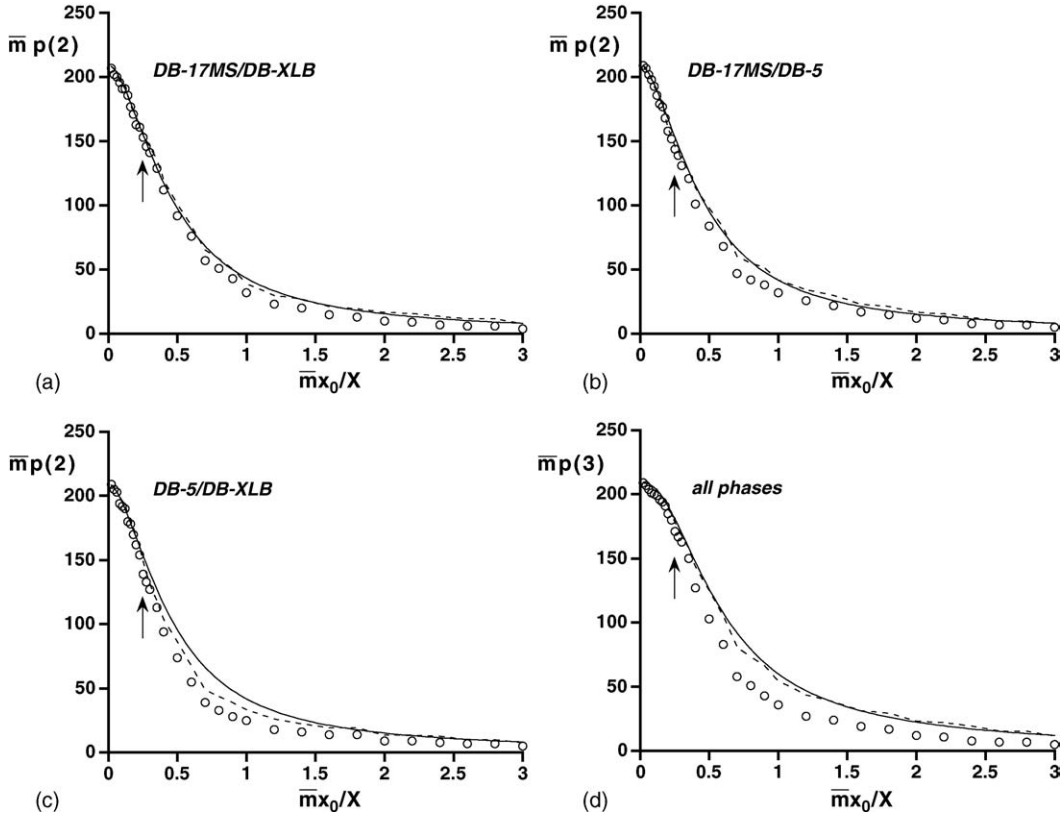

Fig. 5. Graphs of numbers of PCBs expected to be resolved by at least one column vs. $\bar{m}x_0/X$, where x_0 is the minimum interval required for resolution, in (a–c) 2-column separations and a (d) 3-column separation. Circles represent retention-index results; solid and dashed curves represent theory based on SOT and empirical probabilities, respectively. Phase combinations are identified. Arrows identify approximate coordinate corresponding to $x_0 = 1$ index unit.

spans differ slightly (850 for DB-XLB and DB-17MS, 900 for DB-5), the same $\bar{m}x_0/X$ value corresponds to slightly different x_0's. Actually, any combination of x_0's could be used; in the simplest case, however, $\bar{m}x_0/X$ is the saturation and a useful coordinate of comparison. In the graphs, the solid and dashed curves represent theory based on SOT and empirical probabilities, respectively, and the symbols represent results calculated from the retention indices. The two theories agree well, except for DB-5 and DB-XLB over the range, $0.5 < \bar{m}x_0/X < 1.5$, in Fig. 5c, and both agree with the index results for $\bar{m}x_0/X < 0.5$ or so. For larger $\bar{m}x_0/X$, the theory and index results may agree or disagree, depending on the specific case. This is not surprising, since early SOT based on the Poisson distribution explained that the assumption of randomness is most justified in high resolution separations (small x_0), in which minor chemical differences among adjacent components shift peak spacing by several units of resolution [8]. Regarding the errors at large $\bar{m}x_0/X$, we observe that theory overpredicts the singlet numbers, especially for the 3-column separation, due to reinforcement of error on multiplication of $\bar{p}_i$'s. The arrows in the graphs identify the coordinate roughly corresponding to $x_0 = 1$. At this coordinate, the graphed results are similar but not identical to those in Table 3, since x_0 varies slightly in the former. Since this coordinate is about 0.25, accurate predictions are possible for intervals x_0 smaller than about 2 index units.

We observe that one can use theory as a guideline to further improvements of the PCB separation. For example, Eq. (1) predicts that addition of two more independent columns, which also provide p_i's of 0.5, should increase the probability of singlet formation to 0.969, making possible the separation of 202 of the 209 PCBs. As another example, Eq. (1) predicts that improving the existing three separations, such that all p_i's equal 0.7, should achieve about the same result.

4.4. Origin of column independence

Our theory is based on the assumption that all probabilities p_i and $\bar{p}_i$ are independent and can be multiplied to calculate state probabilities. A discussion of this assumption is warranted. Clearly, independence cannot be interpreted as the absence of correlation among retention indices. All the stationary phases considered here are low polarity, and correlations among indices are evident. One correlation is global, in that elution order increases with the number of chlorine atoms. Another correlation is local, in that most PCBs are bracketed by adjacent neighbors that are the same for different columns. Indeed, only 50 of the 209 PCBs are bracketed by immediately adjacent neighbors that differ on all three columns.

Rather, independence implies that a component may or may not be separated by different columns. A simple anal-

ogy clarifies this assertion. Consider that the outcomes of a series of coin tosses represent resolution or lack of resolution of all compounds by a specific column (the probabilities of "heads" and "tails" need not be equal). Consider also that different sequences of coin tosses represent separation attempts by different columns. If independence exists and a probabilistic description is valid, then a compound arbitrarily labeled "5" (e.g., congener 5) cannot always be resolved by all columns, anymore than the fifth coin toss (which also is labeled "5") in different sequences of coin tosses can always turn up "heads". The argument is equally valid, if the coin toss labeled "5" is not actually the fifth toss but a different one (i.e., if the compound elution order is changed among separations). Random outcomes of success and failure of separation must both occur for each compound, in accordance with probabilities p_i and $\overline{p}_i$.

We consider the independence of the PCB p_i's in two-column separations from two perspectives, postulating that the same issues are important for n-column separations in general. First, independence appears to occur because differences between the retention indices of most PCBs on the different phases are much larger than the retention-index interval required for separation. Fig. 6 reports the difference ΔI of retention index versus the IUPAC congener number, where ΔI is the difference between the congener's retention index on two phases. All three ΔI combinations are considered, and the choice of which index is subtracted from the other is arbitrary. The differences essentially are random; the correlation coefficients of lines fit to coordinates in Fig. 6a, b, c are 0.0295, 0.156, and 0.188, respectively. The average $|\Delta I|$ is less than one index unit in all graphs, with standard deviations σ of 12.7, 10.7, and 6.9 in the respective figures. Because of local correlations, many PCBs and their adjacent neighbors have ΔI's that are similar in sign but different in magnitude. Since the assumed retention-index interval required for resolution, as reported in ref. [3], is only one unit – a small fraction of most ΔI's – small and subtle contributions to ΔI are sufficient to cause separation by some phases but not by others. In contrast, if all ΔI's were the same, the same distribution of resolved and unresolved congeners would appear in all separations, independence would be absent, and theory would break down.

To support this argument, we observe that the largest and smallest σ's reported above are associated with the best and worst agreements of index data and theory for the 2-column separations (cf. Figs. 5a and 6a, and Figs. 5c and 6c). Thus, it appears that theory breaks down when the resolution interval x_0 becomes comparable to the spread of ΔI's. In contrast, theory appears to be valid when x_0 is much smaller than the spread of ΔI's.

The above perspective largely is intuitive. A second and more quantitative one is obtained by studying correlation among the intervals x_s governing separation. In most cases, x_s is the smaller of the two intervals between a congener and its adjacent neighbors. For the first or last eluting congener, it is the interval to its single adjacent neighbor. For two adjacent congeners, it actually may be the same interval. These intervals govern separation, since if $x_s \geq x_0$, then a congener is a singlet, whereas if $x_s < x_0$, then a congener is part of a cluster.

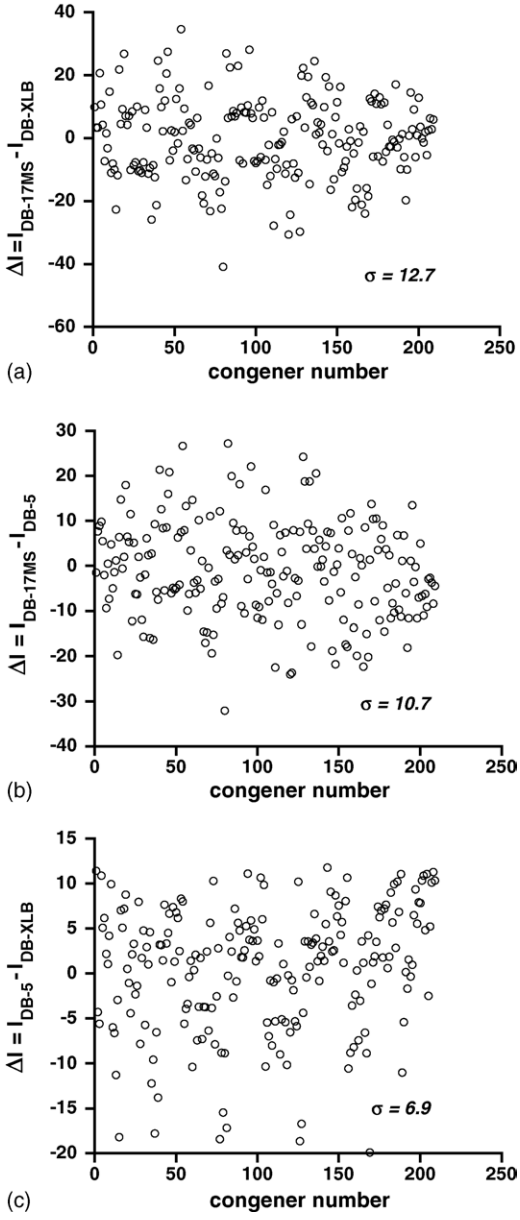

Fig. 6. (a–c) Graphs of differences ΔI between retention indices of PCBs on two columns vs. IUPAC congener number. Phase combinations are identified and identical to those in Fig. 5a–c. Standard deviations, σ of ΔI's are reported.

Fig. 7a is a graph of x_s, as measured in index units, for congeners on the DB-17MS column versus its DB-XLB counterpart, with each coordinate representing a specific congener. Any correlation in this graph, as measured by the linear correlation coefficient r, signifies that congeners do not behave independently on the two columns. This assertion is supported by simulations mimicking the DB-17MS and DB-XLB separations with random retention indices, for which coordinates

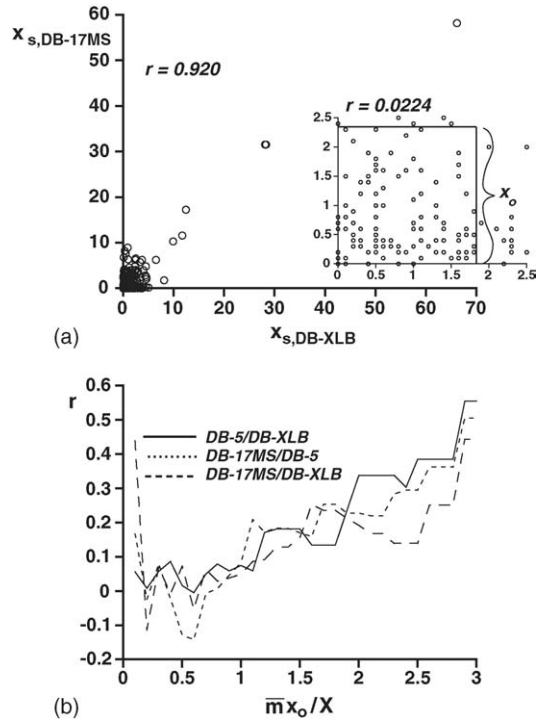

Fig. 7. (a) Graph of intervals x_s on DB-17MS column vs. intervals x_s on DB-XLB column. Insert shows graph for small x_s, with square of dimension x_0 containing coordinates of congeners resolved by neither column at separation threshold x_0. (b) Graph of r vs. $\bar{m}x_0/X$ for the three two-column separations considered in Fig. 5.

in graphs like Fig. 7a have no correlation. Most intervals x_s in Fig. 7a are small, as indicated by the high coordinate density near the origin. In contrast, a few coordinates having large x_s values lie near the diagonal and represent congeners that are well separated by both columns (such coordinates are absent in graphs based on simulations). Most of these congeners are found at the separations' ends, where the density of indices is very low, and only a few of them are needed to cause correlation, as quantified by the large r value (0.920) in the figure.

In contrast, the insert to Fig. 7a is an expansion of the graph for small x_s. These coordinates have some structural location, because indices are known only to 0.1 index units and adjacent congeners can be associated with the same x_s. However, they are largely uncorrelated, as indicated by the small r value (0.0224). It is evident that correlation of the x_s intervals of DB-XLB and DB-17MS is negligible for small x_s but significant for large x_s. The other two-column separations in Fig. 5 behave similarly.

If we consider only probability $p(2)$ and not individual state probabilities, then the amount of independence in our two-column separations appears to be related to the size of separation interval x_0. The insert to Fig. 7a shows a square having dimension x_0. Two sides of the square coincide with the graph axes. The coordinates within the square (i.e., the x_0-square) correspond to congeners that are resolved by neither column, since $x_s < x_0$ for both columns. If probability theory is valid, then the probability that coordinates lie within the square must equal $\bar{p}(2)$. Indeed, the complement of the probability that coordinates lie within the square, as evaluated from 500 simulations of mimicked separations, is exactly equal to the theoretical curve for $p(2)$ in Fig. 5a. Since coordinates in such simulations are not correlated, we propose that the validity of probability theory for $p(2)$ can be gauged by the amount of correlation in the x_0-square, at least to a first approximation. Fig. 7b is a graph of r versus $\bar{m}x_0/X$ for the three two-column separations considered in Fig. 5, with r calculated from coordinates in x_0-squares of various sizes (the square is replaced by a rectangle, when x_0 differs for the two columns). Quantity r does not vary smoothly with $\bar{m}x_0/X$ due to the slightly discretized coordinate locations. With one exception attributable to small numbers of coordinates, r is small for small $\bar{m}x_0/X$ and increases with increasing $\bar{m}x_0/X$. Specifically, correlation is virtually nonexistent for $\bar{m}x_0/X < 0.5$, the range in Fig. 5 over which theory for $p(2)$ is most valid. These findings give some quantitative insight into the agreement and disagreement between index results and theory in Fig. 5 for small and large $\bar{m}x_0/X$, respectively.

The assertion that x_0, which is related only to separation efficiency, is connected to correlation should not be puzzling. In many ways, it is no different from the assertion that SOT is more valid for small x_0 than large x_0.

From these considerations, we conclude that the PCB separations are independent only over a limited range of small x_0. Because of this, our application of theory to them is slightly compromised. Clearly, it would be better if we had independent indices but these are rare. Also, we recognize that other issues may be relevant to the origin of independence and will become more apparent as future studies unfold.

4.5. Limitations of theory

Since many chemical interactions affecting retention are similar for different stationary phases, an upper bound to n must exist, beyond which the assumption of independence breaks down under the best of circumstances. Unfortunately, we cannot predict that number; it depends on both the phases and mixture composition. Clearly, at least three columns can be used, when separation efficiency is high (i.e., x_0 is small). Further study is necessary to evaluate the bound.

Another limitation is that $\alpha_e(n)$, Eq. (4b), cannot be interpreted as the effective saturation of an n-column separation. Rather, as defined after Eq. (3), it is the effective saturation of an n-column separation having the same probability of singlet formation as a single-column separation. Consequently, one cannot predict from $\alpha_e(n)$ the relationships between peaks, doublets, triplets, etc., in single-column and n-column separations.

5. Conclusions

One of the objectives of SOT is to provide quantitative estimates of the likelihood of separation. Our theory pro-

vides guidelines for the method developer who desires low effective saturations, high effective peak capacities, short analysis times, and large linear ranges, without using multi-dimensional separations. By determining p_i, which can be calculated once $\bar{m}$ is estimated by one of several procedures [4–7], the method developer can attain the desired level of separation by improving the existing n-column separation, adding more columns, or doing both.

It is interesting to note that correlations among different columns are far less destructive to a statistical interpretation of n-column separations than of multi-dimensional ones. For example, the use in GC × GC of any of the two columns chosen to measure PCB retention indices would produce (unless unusual programming conditions were chosen) a highly structured and ordered two-dimensional separation, which could not be interpreted by Eq. (10). Although SOT based on autocorrelation methods has progressed toward such an interpretation [10], it remains a complicated problem. It is satisfying to find that simple probabilistic approaches are useful in some aspects of correlated separations.

Finally, it is worth considering that theory also may apply to the same column operated under different conditions, such as a GC capillary that is temperature programmed at different heating rates.

References

[1] K.A. Connors, Anal. Chem. 46 (1974) 53.
[2] M. Martin, D.P. Herman, G. Guiochon, Anal. Chem. 58 (1986) 2200.
[3] S. Chu, C.-S. Hong, Anal. Chem. 76 (2004) 5486.
[4] J.M. Davis, in: P. Brown, E. Grushka (Eds.), Advances in Chromatography, vol. 34, Marcel Dekker, Inc, New York, 1994, p. 109.
[5] A. Felinger, in: P. Brown, E. Grushka (Eds.), Advances in Chromatography, vol. 39, Marcel Dekker, Inc, New York, 1998, p. 201.
[6] A. Felinger, Data Analysis and Signal Processing in Chromatography, Elsevier, Amsterdam, 1998, p. 331.
[7] A. Felinger, M.C. Pietrogrande, Anal. Chem. 73 (2001) 619A.
[8] J.M. Davis, J.C. Giddings, Anal. Chem. 55 (1983) 418.
[9] K. Rowe, J.M. Davis, Anal. Chem. 67 (1995) 2981.
[10] N. Marchetti, A. Felinger, L. Pasti, M.C. Pietrogrande, F. Dondi, Anal. Chem. 76 (2004) 3055.
[11] J.M. Davis, J. Sep. Sci 28 (2005) 347.
[12] J.M. Davis, Anal. Chem. 65 (1993) 2014.
[13] M. Martin, J. Fresenius, Anal. Chem. 352 (1995) 625.
[14] Z. Liu, J.B. Phillips, J. Chromatogr. Sci. 29 (1991) 227.
[15] L.M. Blumberg, J. Chromatogr. A 985 (2003) 29.
[16] W. Bertsch, J. High Resolut. Chromatogr. 22 (1999) 647.
[17] T. Górecki, J. Harynuk, O. Pani, J. Sep. Sci. 27 (2004) 359.
[18] M.M. Bushey, J.W. Jorgenson, Anal. Chem. 62 (1990) 978.
[19] T.F. Hooker, J.W. Jorgenson, Anal. Chem. 69 (1997) 4134.
[20] X. Zhang, H.-L. Hu, S. Xu, X. Yang, J. Zhang, J. Sep. Sci. 24 (2001) 385.
[21] X. Yang, X. Zhang, A. Li, S. Zhu, U. Huang, Electrophoresis 24 (2003) 1451.
[22] W. Shi, J.M. Davis, Anal. Chem. 65 (1993) 482.
[23] J.M. Davis, Anal. Chem. 66 (1994) 735.
[24] C. Samuel, J.M. Davis, J. Chromatogr. A 842 (1999) 65.
[25] J.M. Davis, C. Samuel, J. High Resolut. Chromatogr. 23 (2000) 235.
[26] W.H. Press, S.A. Teukolsky, W. Vetterling, B.P. Flannery, Numerical Recipes in FORTRAN, second ed., Cambridge University Press, Cambridge, UK, 1992, p. 279.
[27] P.J. Marriott, M. Dunn, R. Shellie, P. Morrison, Anal. Chem. 75 (2003) 5532.
[28] R.B. Gaines, G.S. Frysinger, J. Sep. Sci. 27 (2004) 380.
[29] C.M. Harris, Anal. Chem. 74 (2002) 410A.
[30] L.M. Blumberg, Anal. Chem. 74 (2002) 503A.
[31] M.C. Pietrogrande, L. Pasti, F. Dondi, M.H.B. Rodriguez, M.A.C. Diaz, J. High Resolut. Chromatogr. 17 (1994) 839.
[32] C. Samuel, J.M. Davis, J. Microcol. Sep. 12 (2000) 211.